IEEE Access
Multidisciplinary | Rapid Review | Open Access Journal

Received April 28, 2019, accepted June 17, 2019, date of publication June 20, 2019, date of current version July 11, 2019.

Digital Object Identifier 10.1109/ACCESS.2019.2924050

Testing Method for Composite Insulators Interface Based on Nonlinear Ultrasonic

SIDA ZHANG[1], CHENJUN GUO[2], LI CHENG[1], (Member, IEEE), HANQING WANG[1], AND RUIJIN LIAO[1], (Member, IEEE)

[1]State Key Laboratory of Power Transmission Equipment & System Security and New Technology, Chongqing University, Chongqing 400044, China
[2]Yunnan Electric Power Research Institute, China Southern Power Grid, 530100 , China

Corresponding author: Li Cheng (chengl16@cqu.edu.cn)

This work was supported in part by the National Natural Science Foundation of China under Grant 51707020, and in part by the Chongqing Research Program of Basic Research and Frontier Technology under Grant cstc2017jcyjAX0460.

ABSTRACT The interface is the weakness of composite insulators. As the interface bonding fails, the uniform distribution of electric field will be affected, which accelerates the aging of composite insulators and affects the safe operation of transmission lines. Because of the stress between the sheath and the rod, the air gap at the interface is generally less than 10 ţm and there is extrusion contact in some areas. Therefore, conventional nondestructive testing technology based on refraction and reflection principle cannot effectively identify the faulty insulators in the initial stage of bonding failure. Based on the constitutive model of the interface of composite insulators, the friction force of the interface after bonding failure introduces more nonlinearity in mechanical properties than hydrogen bond under well bonding condition. The numerical results show that under the influence of the nonlinear constitutive relation, the higher harmonic components in the spectrum will increase significantly. The experimental results of plate and insulator samples confirm the validity of numerical calculation. Based on the normalized nonlinearity coefficient, the interface state of composite insulators at the initial stage of bonding failure can be effectively identified.

INDEX TERMS Nonlinear ultrasonic, constitutive model, composite insulators, nondestructive testing.

I. INTRODUCTION

Advantaged by light quality and outstanding resistance of contamination flashover, etc., silicone rubber, glass fibre reinforced epoxy resin and other polymer are widely used in electrical equipment, such as sleeve, transformer, insulator and so on [1]–[4]. Influenced by the production process of composite insulators, bonding failure of sheath rod interface is a common hidden danger of composite insulators in transmission lines [5]. When composite insulators are put into operation, the uniform distribution of electric field is affected by interface defects. Under the action of discharge and hydrolysis, the interface defects caused by bonding failure will develop rapidly, which will lead to the corrosion of epoxy resin and the exposure of glass fibers. Because of that, the mechanical strength of composite insulator rods will reduce (Fig.1.a). In recent years, a new type of fracture accident occurs frequently. Existing research shows that this kind of fracture is closely related to the interface defect of composite insulators and it has led to great influence and serious consequence [6], [7]. Therefore, improving the interface quality of composite insulators through effective nondestructive testing is of great significance to the safe operation of power grid.

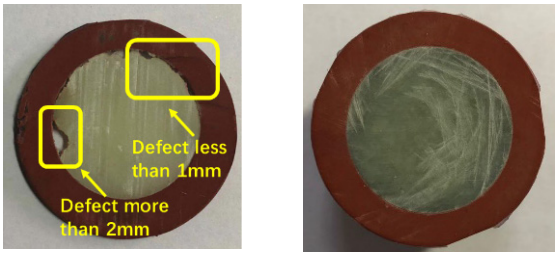

FIGURE 1. Interface defect of composite insulators: (a) Air-gap defect; (b) bonding failure defect.

In recent years, nondestructive testing based on the principle of refraction and reflection, such as electromagnetic wave, infrared thermal wave and ultrasonic wave has been studied in the electrical field, but only the air gap in composite insulators interface as the identification object could be

The associate editor coordinating the review of this manuscript and approving it for publication was Bora Onat.

recognized [8]–[10]. THz time-domain spectroscopy technology can identify air gap defects of 0.4mm or more at the interface of composite insulators using electromagnetic wave as the medium [11]. Active infrared thermal wave detection takes the surface temperature difference caused by interface defects as object [12]. Although it has the advantages of long-distance and high efficiency, the detection accuracy is relatively low. It is difficult to identify defects of 1mm or smaller and recognition ability is affected by the thickness and thermal conductivity of surface materials. Conventional ultrasonic technology has been used in electrical field for a long time, while only the size of air gap can be recognized to a certain extent [8], [9], [13]. However, before the corrosion of epoxy resin, due to the strong flexibility of the silicone rubber used in composite insulators and unique cylindrical structure, the two materials at the interface exist in the form of extrusion contact under the action of internal stress (Fig.1.b). In the existing national standards, the bonding performance of composite insulator interface is evaluated by the results of sample dissection and aging resistance test [14], [15]. There is no effective nondestructive testing scheme for adhesion property. Therefore, the nondestructive testing research of interface bonding performance for composite external insulation equipment has important engineering value in the electrical field.

Over the years, a great deal of achievements have been made in bonding quality evaluation based on the nonlinearity of ultrasonic echo, and it has been successfully applied to the bonding detection of metal materials [16]–[20]. The results of existing nonlinear acoustic studies show that the fatigue of the adhesive layer itself or the breakage of the chemical bond between the adhesive and adherend are the fundamental factors causing the nonlinear distortion of the interface wave [21]–[24]. The theoretical model provides a basis for the application of non-linear ultrasound, but the testing object is limited to the bonding structure with macroscopic bonding layer. However, the adhesive layer of composite insulators is not more than 1.2 um under normal conditions and the sheath material itself contains large nonlinearity compared with metal materials [25]. Based on the interface microstructure of composite insulators, the nonlinearity of the polymer materials interface is described by constitutive model which not only realize the bonding performance evaluation of composite insulators, but also broaden the application field of nonlinear ultrasonic testing.

Firstly, the bonding mechanism and microstructure of composite insulator interface are studied and observed. The hydrogen bond spring model and hysteretic friction model are introduced into the mechanical wave propagation process. The interfacial mechanical properties of different bonding states are equivalent described as corresponding mechanical equations. Then, the excitation source is introduced into the mechanical model and the overall structure of the testing equipment and the sample is described by oscillator model and corresponding equations. On the basis of that, an ultrasonic testing platform is built to detect and analyze the bonding performance of plate and insulator samples based on model parameters. The experimental results show that as the contact force exists, the harmonic components of ultrasonic echo in bonding failure samples increase significantly, which is consistent with the solution of wave equation. Finally, the normalized nonlinearity coefficient is used as the parameter to identify the bonding performance of the interface.

TABLE 1. Basic information of the samples.

No.	Type	Polish	Adhesive
1	Plate [1]	Polished	Chemlok-608
2	Plate [1]	Polished	None
3	Plate [1]	Without polish	None
4	Insulator [2]	Polished	Chemlok-608
5	Insulator [2]	Polished	1/2 concentration
6	Insulator [2]	Polished	1/4 concentration
7	Insulator [2]	Polished	Water

II. STUDY ON INTERFACE OF COMPOSITE INSULATOR

The high temperature vulcanized silicone rubber (HTV) and glass fiber reinforced epoxy resin used in composite insulators are typical organic composites. The properties of coupling agent and the treatment craft of interface are important factors affecting the bonding performance. In the production process of composite insulators, cylindrical glass fiber reinforced epoxy resin rod is polished to increase its surface roughness, then liquid silane coupling agent is applied on the surface. The raw rubber is directly vulcanized on the surface of rod by injection vulcanizing machine at 14-16 MPa and 130-150 °C [26]. Under the action of high temperature, high pressure and coupling agent, in addition to the internal cross-linking reaction and the formation of a stable network structure, silicone rubber will form a well bonding interface with epoxy resin with variety of chemical bonds. In order to study the bonding performance of composite insulator interface, the vulcanization temperature and pressure of composite insulator were set as 10°C and 15 MPa, and vulcanization time was 30 set as minutes. plate and short insulator samples were prepared by plate vulcanizer and injection vulcanizer respectively. In order to change the roughness of the interface, some plate samples were polished according to the standard before vulcanization, while others remained smooth. Chemlok-608 was used as an adhesive in the preparation of experimental samples. The adhesives were first prepared according to the instructions and then diluted to one-half and one-quarter of the standard concentration to simulate different failure states. Water was used as the complete failure adhesives. Seven different types of samples are shown in Table 1. Two samples were made with same condition.

Because of the transparency of FRP plate, the interface can be observed directly from the side of FRP plate. For sample No.3, visible air gap appeared at the interface due to bonding

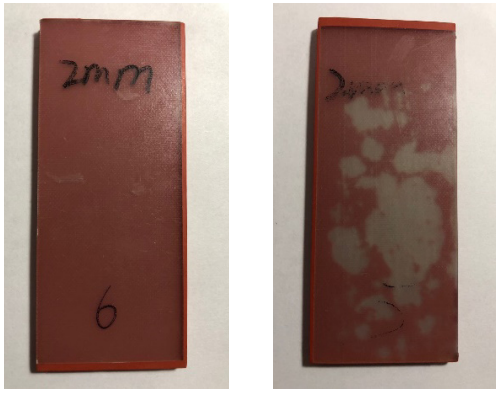

FIGURE 2. Plate samples with different defects: (a) bonding failure defect in No.2 sample, (b) air-gap defect in No.3 sample.

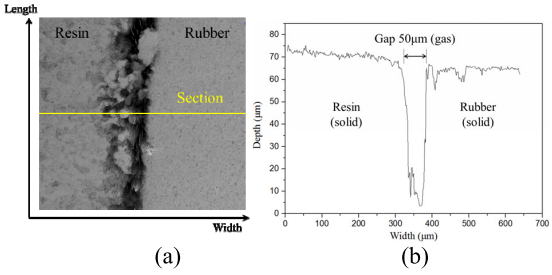

FIGURE 3. The interface micrograph and air gap size of No.3 sample: (a) interface micrograph, (b) air gap size description.

failure and the maximum air gap area is more than 0.25 mm^2. There is no visible defect at the interface of sample No.2 and the appearance of sample No.2 is as same as well bonding sample No.1.

In order to further study the microstate of the interface, laser scanning confocal microscopy (LSCM) was used to characterize the defect of samples quantitatively. The interface micrograph and air gap size of the sample are described in Fig.3.

The interfacial air gap defects in sample No.3 are clearly visible under optical microscopic images. Confocal principle is used to scan the depth section of the selected position to quantitatively analyze the size of air gap at the interface. The results of scanning analysis show that the average thickness of air gap of sample No. 3 is about 50μm, and the maximum is not more than 100μm. For the well bonding sample No.1 and the polished sample No.2, the thickness of the gap layer is not more than 10μm, so that more accurate microscope is needed to observe. The detection accuracy of metallographic microscope can reach 1μm. The microscopic imaging results of No.1 and No.2 samples are shown in Fig. 4. The chemical reaction between silicone rubber and epoxy resin in sample No. 1 make it as a whole, while there is obvious gap between silicone rubber and epoxy resin at No. 2 sample. The size of gap is less than 10um. Influenced by the stress between materials and the roughness of the interface, there is

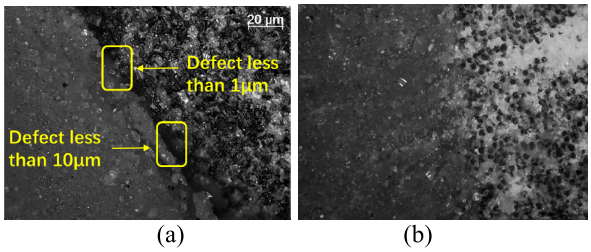

FIGURE 4. Interface microscopic imaging by metalloscope: (a) bonding failure interface in No.2, (b) Normal interface in No.1.

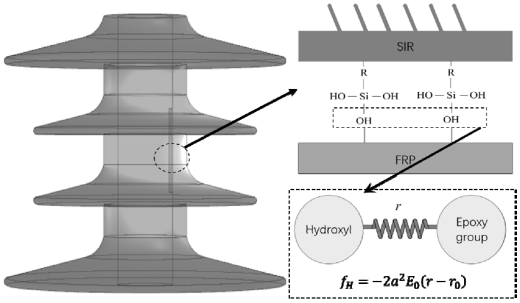

FIGURE 5. Equivalent model for hydrogen bond at interface.

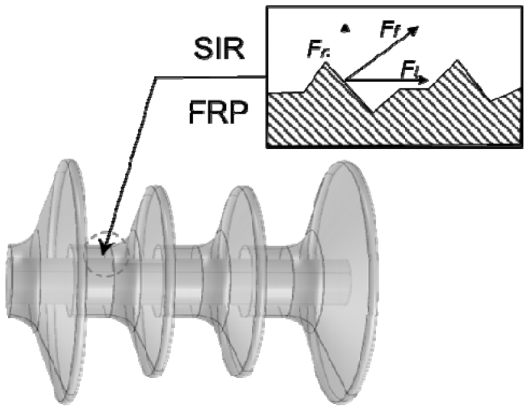

FIGURE 6. Direction of friction in bonding failure interface.

extrusion contact between silicone rubber and epoxy resin at the interface of sample No.2.

III. CONSTRUCTION AND SOLUTION OF CONSTITUTIVE MODEL

A. CONSTRUCTION OF CONSTITUTIVE MODEL

The results of metallographic microscope show that the silicone rubber and epoxy resin in the well bonding samples are formed as a whole through chemical reaction. The bonding force between the two materials is mainly formed by a variety of intermolecular forces, among which the hydrogen bond with the interaction energy of more than 40 kJ/mol is considered to be the main contributor to the interfacial bonding force according to [27]. Hydrogen bond is formed by epoxy ring in epoxy resin as acceptor and hydroxyl group of silicone rubber as donor. The interaction potential

in hydrogen bonds can be described by Morse pair potential [27].

$$E = E_0\left[e^{-2a(r-r_0)} - 2e^{-a(r-r_0)}\right] \tag{1}$$

In (1), E is the interaction energy when the bond length of hydrogen bond is r. a and r_0 are potential trap width and equilibrium bond length of hydrogen bond respectively. Angstrom is used here as the unit of length. If higher order small quantity is neglected, the hydrogen bond force expanded in power series near the equilibrium bond length r_0 could be described as (2).

$$\begin{aligned} f_H &= -\frac{dE}{dr} \approx 2aE_0\left[-2a(r-r_0) + a(r-r_0)\right] \\ &= -2a^2E_0(r-r_0) = -k(r-r_0) \end{aligned} \tag{2}$$

Based on (2), the force in a hydrogen bond is equivalent to the spring force whose original length is r_0 and the elastic constant is $k = 2a^2E_0$. Therefore, the mechanical properties of the well bonding area can be equivalent to the linear hydrogen bond spring model.

Due to the insufficient of adhesives in the production process, the bonding structure between silicone rubber and epoxy resin in some areas change from chemical bonding to extrusion contact. Because the surface of epoxy resin is rough, the viscoelastic silicone rubber and the surface of epoxy resin will produce friction under internal stress.

Although both friction (vertical component) and hydrogen bond forces provide the force needed to maintain interfacial bonding to some extent, only friction has hysteresis. Therefore, the friction makes the stress and strain no longer present a linear relationship, but a hysteretic nonlinear relationship. The bilinear model is suitable for the hysteretic friction phenomenon of rubber materials which is used to explain the nonlinear stress-strain relationship in bonding failure interface [28], [29]. Under the excitation of mechanical waves, the mathematical equation of bilinear model can be expressed as (3)

$$f(\theta) = \begin{cases} k_d(x - A + \mu N), & (0 \le \theta \le \theta^*) \\ -\mu N, & (\theta^* < \theta < \pi) \\ k_d(x - A + \mu N), & (\pi \le \theta \le \theta^* + \pi) \\ \mu N, & (\theta^* + \pi < \theta < 2\pi) \end{cases}$$

$$\theta = \omega t - \varphi \quad \theta^* = \cos^{-1}(1 - \frac{2\mu N}{k_d A}) \tag{3}$$

In (3), k_d is the shear stiffness of the contact surface, x is the relative displacement between the contact surfaces, μ is the friction coefficient of the contact surface, A is the maximum relative displacement between the two contact surfaces, N is the positive pressure between the contact surfaces, ω is the excitation frequency and φ is the phase difference. θ is the excitation phase, θ^* is the phase boundary between the elastic part and the hysteretic part.

$$f\ (\theta) = F_x(A)\cos\theta + F_y(A)\sin\theta \tag{4}$$

When the relative motion of two contact surfaces is harmonic, (3) is transformed to (4) by harmonic balance method.

$$\begin{aligned} F_x &= \frac{2}{\pi}\int_0^{\pi} f\cos\theta d\theta = \frac{k_d A}{\pi}\left(\theta^* - 0.5\sin 2\theta^*\right) \\ &= \frac{k_d A}{\pi}\left[\cos^{-1}\left(1 - \frac{2\mu N}{k_d A}\right) - 0.5\sin 2\left(1 - \frac{2\mu N}{k_d A}\right)\right] \\ F_y &= \frac{2}{\pi}\int_0^{\pi} f\sin\theta d\theta = -\frac{4}{\pi}\mu N\left(1 - \frac{\mu N}{k_d A}\right) \end{aligned} \tag{5}$$

Equation (5) is an expansion of F_x and F_y, which are functions of A or θ.

$$\begin{aligned} f(\theta) &= k_e A\cos\theta + c_e\omega A\sin\theta \\ k_e &= \frac{F_x(A)}{A} c_e = \frac{F_y(A)}{\omega A} \end{aligned} \tag{6}$$

Equation (6) is further deduced from (4). In the equation, k_e is equivalent stiffness and c_e is equivalent damping.

$$f(t) = k_e x(t) + c_e\frac{dx(t)}{dt} \tag{7}$$

The mechanical properties of the model can be explained clearly by converting friction into function of time. The elastic force is proportional to the displacement of the interface and the viscous force is proportional to the velocity of the interface which present linear and nonlinear respectively and the degree of which can be expressed by equivalent stiffness k_e and equivalent damping c_e. Therefore, when the bonding fails, the friction between the two materials will increase the nonlinear component of the whole system.

B. SOLUTION OF CONSTITUTIVE MODEL

Different bonding states of interfaces are equivalent described as corresponding mechanical equations of hydrogen bond spring model and hysteretic friction model. However, the solution of wave equation requires the introduction of excitation source and considers the overall structure of sound wave transmission process. In order to realize the solution of the model, the oscillator model and equations are introduced to describe the whole structure of the testing equipment and samples.

The oscillator model is shown in Fig.7 which is constructed from the bottom to the top. The bonding interface is composed of silicone rubber and glass fiber reinforced epoxy resin. The deformation of glass fiber reinforced epoxy resin at the bottom of the bonding interface is extremely weak so that it is considered as a rigid body in this model. The sheath thickness of silicone rubber material is basically the same in the sample. So the thickness of the silicone rubber layer is neglected in the model and only equivalent mass characteristics M_2 are retained.

$$M_2 = \rho \times S_2 \times d \tag{8}$$

In (8), ρ is the density of silicone rubber and d is the thickness of interface. S_2 is the equivalent area of the interface, which is related to the surface roughness R_a of the polished rod and the depth d_R of the polished microcrack.

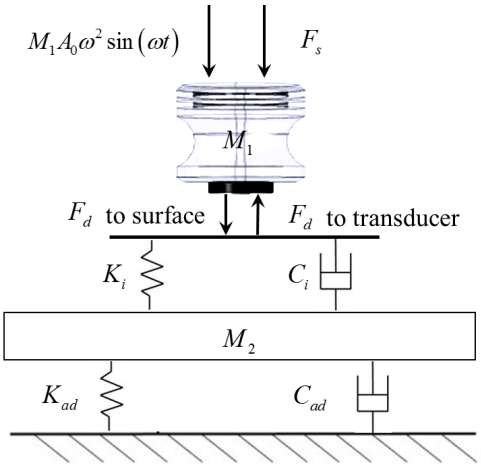

FIGURE 7. Interface oscillator model.

Preliminary assumption is that the rough ''particles'' on the surface of the polished rod are cuboids and the value of S_2 can be estimated by (9).

$$S_2 = \frac{4S_1}{(2R_a)^2} \cdot d_R \cdot R_a = \frac{d_R}{R_a} S_1 \tag{9}$$

In (9), S_1 is the effective detection area of the ultrasonic transducer. For well bonding samples, the hydrogen bond spring model is used as the prototype and the elastic constant is K_{ad1}.

$$K_{ad1} = E_{ad} \times S_1 \tag{10}$$

According to the data provided by the manufacturer, the elastic modulus E of silicone rubber is 9.4 MPa. For well bonding interface, its elastic modulus E_{ad} is four times that of material elastic modulus E [30]. Since there is no nonlinear component, the damping coefficient C_{ad1} is set to zero.

$$K_{ad2} = G \times S_2 \tag{11}$$

For bonding failure samples, hysteretic friction model should be used for analysis. The elastic constants depend on the shear modulus of silicone rubber G and equivalent area of the bonding interface S_2 [30]. Referring to the range of nonlinear friction damping of macromolecule materials, the value of damping coefficientC_{ad2} at failure bonding interface is 500 N·s/m [28]. The piezoelectric wafer of the ultrasonic transducer acts as an excitation source (its equivalent mass is M_1) is coupled with silicone rubber by coupling agent under the action of external pressure F_s. Nonlinear contact damping model is introduced to describe the behavior of contact force F_d [31]. To ensure that the contact force F_d can continuously change, which is expressed as (12).

$$F_d = \begin{cases} K_i X_1(t) + C_i \dfrac{dX_1(t)}{dt} & (X_1 \geq 0) \\ 0 & (X_1 < 0) \end{cases} \tag{12}$$

In (11), K_i is equivalent contact stiffness and C_i is equivalent contact damping. The absolute values of the contact force parameters K_i and C_i cannot be obtained directly by theoretical calculation or experiment. While the ratio range of K_{ad}/K_i and C_{ad}/C_i in the simulation model can be deduced by experimental results and the specific ratio can be determined according to the material [32]–[34]. K_{ad}/K_i and C_{ad}/C_i are 167 and 500 respectively for contact epoxy resin and silicone rubber materials. The simulation parameters of the collision oscillator model are shown in Table 2.

TABLE 2. Simulation parameters of the collision oscillator model.

Parameter	Well Bonding	Bonding failure
Equivalent mass of ultrasonic transducer M_1	0.03kg	0.03kg
Equivalent mass of interface M_2	0.011kg	0.011kg
Elastic constant K_{ad}	7144 N/m	5969 N/m
Damping coefficient C_{ad}	0 N/m	500 N/m
External pressure F_s	10 N	10 N

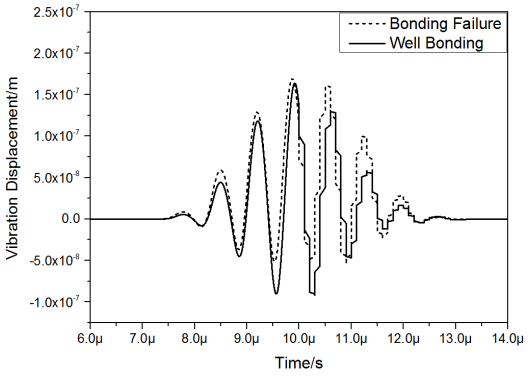

FIGURE 8. Simulation results of oscillator model: Waveform in time domain.

The oscillator model combined with source excitation is described by (13) and then solved by Runge-Kutta method in MATLAB.

$$\begin{cases} M_1 \dfrac{d^2X_1}{dt^2} = F_s + M_1A_0\omega^2\sin(\omega t) - F_d \\ M_2 \dfrac{d^2X_2}{dt^2} = F_d - C_{ad}\dfrac{dX_2}{dt} - K_{ad}X_2 \end{cases} \tag{13}$$

In order to ensure that the excitation function is consistent with the output of the transducer, excitation frequency ω is set as 3×10^6 rad/s and amplitude A_0 is processed by Hanning window with 10 cycles. The displacement X_1 of the piezoelectric wafer is taken as an unknown variable to solve shown in Fig.8.

It can be found that the displacement X_1 of piezoelectric wafer distorts when the interface bonding fails, but the phase does not shift. The FFT module is used to convert the solution as frequency and the spectrum of vibration waveform is obtained shown in Fig.9. Compared with the time domain waveform, the difference between the two models in the

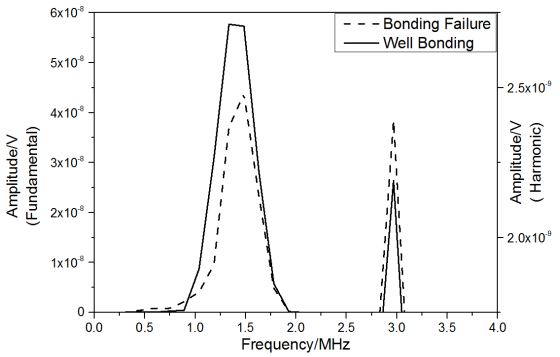

FIGURE 9. Simulation results of oscillator model: Spectrum in frequency domain.

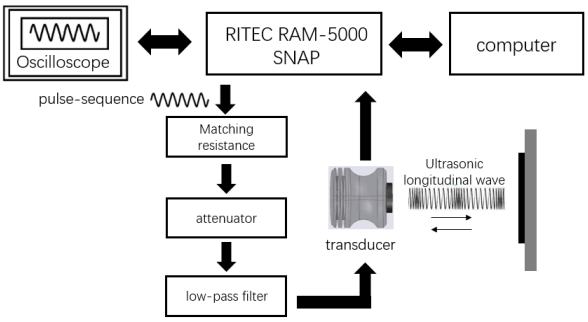

FIGURE 10. Working principle of the ultrasonic system.

spectrum is more obvious. The increase of nonlinear factors leads to the decrease of fundamental wave and the rise of second harmonic. In other words, spectrum energy transfer to higher harmonic as bonding failure.

IV. TESTING METHOD AND EXPERIMENTAL SYSTEM

The ultrasonic system consists of RITEC RAM-5000 SNAP, matched resistance, attenuator, low-pass filter, ultrasonic transducer, fixing and counterweight device, which is shown in Fig.10. The parameters of excitation frequency, pulse width and excitation energy are set according to simulation parameters. Longitudinal wave probe produced by Olympus Corporation (V106) was used in ultrasonic experimental system with 2.25 MHz as central frequency and bandwidth meeting requirements. It also has high gain for the fundamental frequency of 1.5 MHz and the second harmonic frequency of 3.0MHz.

The coupling degree between transducer and sample plays a crucial role in the experimental results. The additional nonlinear factors will result in non-tight coupling condition so that the accuracy and robustness will be lost. In addition to the using of small nonlinear coupling agent, transducer fixture is used to provide the pressure needed for coupling in the experiment to ensure that the coupling degree is sufficient and constant (Fig.11.a). For the cylindrical sample, the arc surface is difficult to fully contact with the probe so that the effective incidence of ultrasonic cannot be achieved only by coupling agent. The wedge is made of nonlinear minimal PPS plastic to realize the tight coupling between the probe and the tested sample (Fig.11.b).

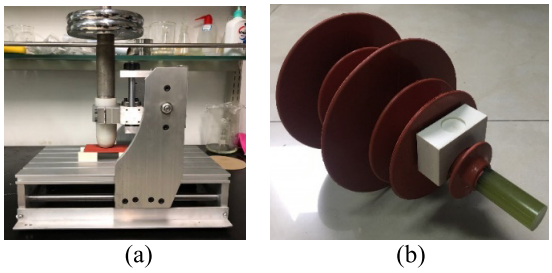

FIGURE 11. Device for ensuring coupling degree: (a) Test platform and counterweight, (b) Insulator sample and wedge.

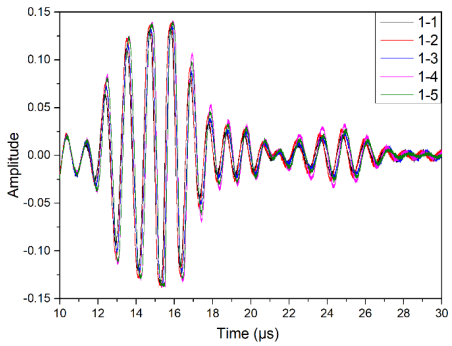

FIGURE 12. Waveform of sample No.1 in time domain.

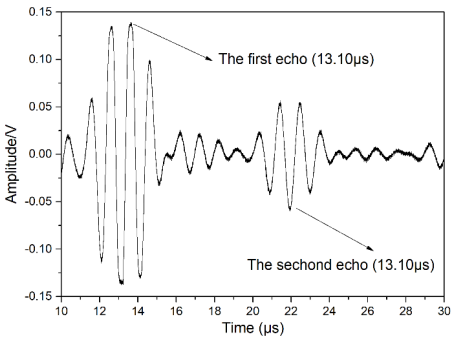

FIGURE 13. Waveform of sample No.3 in time domain.

V. RESULTS AND DISCUSSION

A. ANALYSIS OF RESULTS IN TIME DOMAIN

The echo signal waveform of sample No.1 received by the transducer in time domain is shown in Fig.12. It can be seen that the waveform of the well bonded sample is consistent.

The echo signal waveform of sample No.3 is completely different from that of sample No.1 when the continuous air-gap layer appears (Fig.13).

The appearance of such waves comes from the isolation of acoustic waves by air-gap. Because of the significant difference of acoustic impedance between gas and solid, the incident acoustic wave cannot penetrate the air-gap layer. The completely reflection of incident acoustic wave in the air-gap layer causes the change of waveform in time domain. For such time domain waveforms, it can be analysed by acoustic reflection theorem, which has been widely used in the detection of internal defect of equipment. The thickness

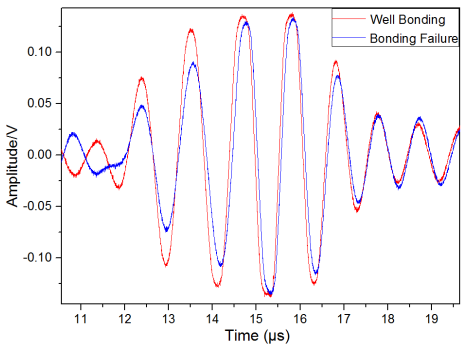

FIGURE 14. Waveform of sample No.1 and No.2 in time domain.

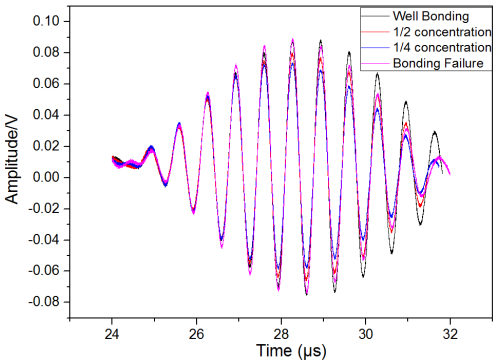

FIGURE 15. Waveform of sample No.4 to No.7 in time domain.

of the surface material can be calculated according to the time of two echoes and the acoustic velocity in the silicone rubber material, which is consistent with sample thickness.

Compared with No.3 sample, the surface roughness of No.2 is improved greatly by polish. On this condition, silicone rubber contacts with epoxy plate fully during vulcanization process and forms extrusion contact under stress after cooling which effectively avoids the formation of air gap layer. Therefore, the time domain waveform of sample No.2 are only slightly different from that of sample No.1 in amplitude (Fig.14), which is consistent with the numerical results of the constitutive model. However, in the actual detection process, the waveform distortion caused by the interface is difficult to distinguish due to the influence of coupling conditions and detection location.

The waveform of cylindrical samples are shown in Fig. 15. It can be found that changes in the concentration of adhesives, i.e. changes in the number of hydrogen bonds at the interface, can also distort the waveform in time domain, and the distortion in time domain occurs more frequently in the latter half of the waveform, which is consistent with the results of numerical calculation.

B. ANALYSIS OF RESULTS IN FREQUENCY DOMAIN

Using the same FFT model in MATLAB software, the time-frequency conversion of the experimental ultrasonic echo signals are shown in Fig.16. According to the spectrum obtained from the experiment, the difference is very small in the fundamental wave, while the difference in the second harmonic wave is obvious.

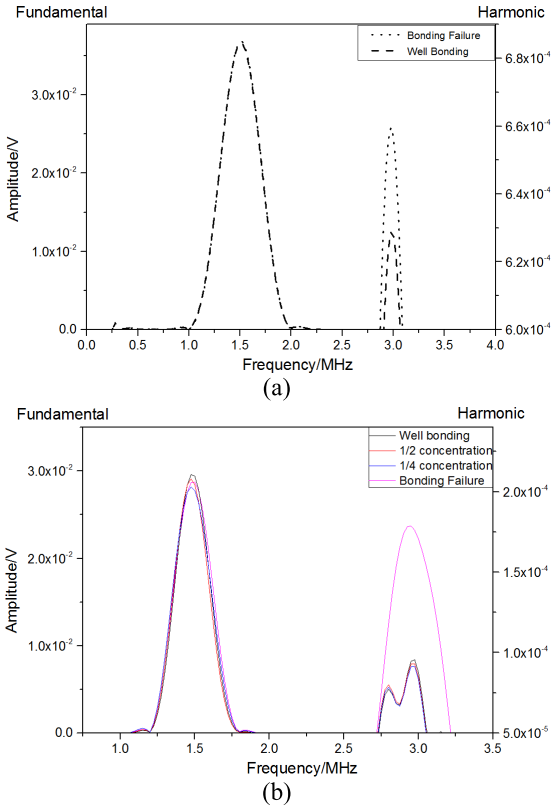

FIGURE 16. Spectrum of nonlinear ultrasonic testing results: (a) Spectrum of plate sample, (b) Spectrum of insulator sample.

Well Bonding and bonding failure can be distinguished by second harmonic amplitude, while the change of hydrogen bond density caused by partial failure of adhesives can hardly be identified by spectrum change. The experimental and numerical spectra are consistent in the trend of second harmonic variation but there are some differences in the fundamental wave. This is because the nonlinearity of composite material itself is neglected in numerical calculation. On the other hand, C_{ad} is difficult to set values accurately and the sensitivity of the calculated results to the variation of parameters leads to a certain difference between the calculated and the experimental results. In the next research, we will focus on the change of hydrogen bond density and the roughness of the interface to improve the existing hydrogen bond spring model and hysteretic friction model, so as to achieve quantitative evaluation of interface state.

C. EFFECTIVE CHARACTERIZATION OF COMPOSITE INSULATORS INTERFACE

For the same kind of samples, the ratio of second harmonic amplitude A_2 to fundamental wave amplitude square A_1^2 is more convenient to reflect the information of second-order and third-order elastic constants as the wave number k and the interface position x are constant. So the definition of nonlinear coefficient is set as (14) [35].

$$\beta = \frac{A2}{A_1^2} = \frac{\left(3 + \frac{C_{111}}{C_{11}}\right) k^2 x}{8} \tag{14}$$

TABLE 3. Normalization results of nonlinear coefficients.

Adhesion condition	Plate sample		Insulator sample	
	β'	Variance	β'	Variance
Well bonded	0.78	0.063	0.83	1.469
	0.29		2.08	
	0.67		3.83	
	0.23		3.33	
	0.68		1.76	
Weak adhesive	8.39	0.699	8.01	1.143
	7.90		9.21	
	7.83		7.17	
	9.33		9.23	
	9.66		7.01	

In (14), C_{11} and C_{111} is the second and third Brugger elastic constants of isotropic solid materials respectively written as Voigt symbols here. It is not only of definite physical significance, but also of practical value in engineering to evaluate the interface bonding state by nonlinear coefficient as the detection parameter. The fundamental amplitude A_1 and the second harmonic amplitude A_2 of the reflected signal can be extracted from the spectrum to calculate the nonlinear coefficient β. Furthermore, linear normalization of the measurement results of β is carried out. If β_m is the experimental result of a certain measurement point and there are N measurement points, the linear normalization processing result β' is (15)

$$\beta' = \frac{\beta_m - (\min\{\beta_1, \beta_2, \cdots \beta_N\} - \Delta)}{\max\{\beta_1, \beta_2, \cdots \beta_N\} - \min\{\beta_1, \beta_2, \cdots \beta_N\}} \quad (15)$$

In (15), the existence of Δ enables normalization to be applied to many of the same results which simplifies the calculation steps. The experimental results of linear normalization are shown in Table 3.

Compared with the experimental results of the nonlinear coefficient between the cylindrical and plate structure, the nonlinear coefficient of the bonding failure interface is obviously improved. For well bonding samples, the normalization nonlinear coefficient β' of cylindrical structure is less than 4 and that of plate structure is less than 1. The normalization nonlinear coefficients β' of the bonding failure samples are greater than 7. With a certain margin, $\beta' = 5$ can be used as the boundary value between the bonding failure defect and the well bonding interface in all experimental samples. The experimental results are consistent with the theoretical analysis, which confirms the application validity of nonlinear coefficient to evaluate the adhesive quality for composite insulators.

VI. CONCLUSIONS

The manuscript has elucidated a type of NDT method based on nonlinear ultrasonic to identify bonding failure in composite insulators. As proved by research results:

- The interfacial bonding defects of composite insulators may be caused by the absence of polish process and the failure of coupling agent. The absence of polish process makes the interfacial separation. The separation area is more than 0.25mm^2 and the distance between the two materials is more than 50μm. The thickness of the interface defect caused by the failure of coupling agent is less than 10um and some areas are in the form of extrusion contact.
- Hydrogen bond spring model and hysteretic friction model can be used to describe the well bonding and bond failure interface respectively. Compared with the hydrogen bond spring model, the hysteretic friction model introduces more nonlinear mechanical components. The numerical and experimental results show that nonlinear components lead to the distortion in time domain and change of second harmonic amplitude in the frequency-domain waveform.
- Normalized nonlinear coefficient can be used to analyze the interface state of composite insulators.$\beta' = 5$ can be used as the boundary value between the bonding failure defect and the well bonding interface in all experimental samples.

REFERENCES

[1] X. Liang, S. Wang, J. Fan, and Z. Guan, "Development of composite insulators in China," *IEEE Trans. Power Del*, vol. 6, no. 5, pp. 586–594, Oct. 2015. doi: 10.1109/94.798115.
[2] S. M. Gubanski, "Modern outdoor insulation–concerns and challenges," *IEEE Elect. Insul. Mag.*, vol. 21, no. 6, pp. 5–11, Nov./Dec. 2005. doi: 10.1109/mei.2005.1541483.
[3] E. A. Cherney, "50 years in the development of polymer suspension-type insulators," *IEEE Elect. Insul. Mag.*, vol. 29, no. 3, pp. 18–26, May 2013. doi: 10.1109/mei.2013.6507410.
[4] X. Zhang, J. Zhu, S. Bu, Q. Li, V. J. Terzija, and S. M. Rowland, "The development of low-current surface arcs under clean and salt-fog conditions in electricity distribution networks," *IEEE Access*, vol. 6, pp. 15835–15843, 2018. doi: 10.1109/ACCESS.2018.2806885.
[5] F. Zhang, L. Song, R. Li, and G. Wang, "Evaluation method of defect and fracture reason for composite insulator," *High Voltage Eng.*, vol. 38, no. 11, pp. 3093–3100, 2012.
[6] X. Liang, W. Bao, and Y. Gao, "Decay-like fracture mechanism of silicone rubber composite insulator," *IEEE Trans. Dielectr. Electr. Insul.*, vol. 25, no. 1, pp. 110–119, Feb. 2018. doi: 10.1109/tdei.2018.006773.
[7] B. Lutz, L. Cheng, Z. Guan, L. Wang, and F. Zhang, "Analysis of a fractured 500 kV composite insulator–identification of aging mechanisms and their causes," *IEEE Trans. Dielectr. Electr. Insul.*, vol. 19, no. 5, pp. 1723–1731, Oct. 2012. doi: 10.1109/TDEI.2012.6311521.
[8] C.-Z. Xie, Y. Zhang, Y.-P. Hao, X.-Y. Yuan, and Q.-H. Wei, "Application of ultrasonic flaw detector to internal defects in composite insulators," *High Volt. Eng.*, vol. 35, no. 10, pp. 2464–2469, 2009.
[9] C. Xie, Z. He, Y. Ling, L. Li, F. Zhang, and R. Li, "Using ultrasonic phased array to inspect the internal defects of composite insulators," *Proc. CSEE*, vol. 32, no. s1, pp. 63–68, 2012.
[10] Y. Zhai, R. Chen, Q. Yang, X. Li, and Z. Zhao, "Insulator fault detection based on spatial morphological features of aerial images," *IEEE Access*, vol. 6, pp. 35316–35326, 2018. doi: 10.1109/ACCESS.2018.2846293.
[11] L. Cheng, L. Wang, H. Mei, Z. Guan, and F. Zhang, "Research of nondestructive methods to test defects hidden within composite insulators based on THz time-domain spectroscopy technology," *IEEE Trans. Dielectr. Electr. Insul.*, vol. 23, no. 4, pp. 2126–2133, Aug. 2016. doi: 10.1109/tdei.2016.7556487.
[12] S. Zhang, C. Guo, L. Cheng, and H. Wang, "A far-field evaluation method for interfacial defects existed in composite insulators based on transient thermal wave," *IEEE Access*, vol. 7, pp. 1920–1926, Nov. 2018. doi: 10.1109/ACCESS.2018.2883367.

[13] C. Yuan, C. Xie, L. Li, F. Zhang, and S. M. Gubanski, "Ultrasonic phased array detection of internal defects in composite insulators," *IEEE Trans. Dielectr. Electr. Insul.*, vol. 23, no. 1, pp. 525–531, Feb. 2016. doi: 10.1109/tdei.2015.005225.
[14] *GB/T 22079-2008 Polymeric Insulators for Indoor and Outdoor Use With a Nominal Voltage >1000V-General Definitions, Test Methods and Acceptance Criteria*, China Standards Publishing House, Beijing, China, 2008.
[15] *GB/T 19519-2014 Insulators for Overhead Lines Composite Suspension and Tension Insulators for A.C. Systems With a Nominal Voltage Greater Than 1000V Definitions, Test Methods and Acceptance Criteria*, China Standards Publishing House, Beijing, China, 2014.
[16] M. A. S. Geesey, B. Aristorenas, T. J. Ulrich, and C. M. Donahue, "Investigation of the nonlinearity of transducer acoustic couplants for nonlinear elastic measurements," *NDT E Int.*, vol. 104, pp. 10–18, Jun. 2019.
[17] J. Alston, A. Croxford, J. Potter, and P. Blanloeuil, "Nonlinear non-collinear ultrasonic detection and characterisation of kissing bonds," *NDT E Int.*, vol. 99, pp. 105–116, Oct. 2018.
[18] S. Dahmen, "Influence of volumic fraction of adhesive in elastic and viscous thin bonded aluminum/adhesive/aluminum plate on Lamb modes that have ZGV modes," *Ultrasonics*, vol. 94, pp. 37–49, Apr. 2019.
[19] T. Ju, J. D. Achenbach, L. J. Jacobs, and J. Qu, "Nondestructive evaluation of thermal aging of adhesive joints by using a nonlinear wave mixing technique," *NDT E Int.*, vol. 103, pp. 62–67, Apr. 2019.
[20] G. Shui, Y.-S. Wang, P. Huang, and J. Qu, "Nonlinear ultrasonic evaluation of the fatigue damage of adhesive joints," *NDT E Int.*, vol. 70, pp. 9–15, Mar. 2015.
[21] J. D. Achenbach and O. K. Parikh, "Ultrasonic analysis of nonlinear response and strength of adhesive bonds," *J. Adhes. Sci. Technol.*, vol. 5, no. 8, pp. 601–618, 2010.
[22] M. Rothenfusser, M. Mayr, and J. Baumann, "Acoustic nonlinearities in adhesive joints," *Ultrasonics*, vol. 38, pp. 322–326, Mar. 2000.
[23] G. Liu, J. Qu, L. J. Jacobs, and J. Li, "Characterizing the curing of adhesive joints by a nonlinear ultrasonic technique," in *Review of Progress in Quantitative Nondestructive Evaluation*, vol. 18. New York, NY, USA: Plenum Press, 1999, pp. 2191–2199.
[24] Z. Tang, A. Cheng, and J. D. Achenbach, "An ultrasonic technique to detect nonlinear behavior related to degradation of adhesive bonds," in *Review of Progress in Quantitative Nondestructive Evaluation*, vol. 17. New York, NY, USA: Plenum Press, 1998.
[25] L. X. H. Xiaodong and Z. Fulin, "Selection of composite insulator mandrel and umbrella interface adhesive selection and bonding process determination," *Insulators Surge Arresters*, vol. 6, pp. 7–13, 2012.
[26] X. Li and X. Han, "Selection of composite insulator mandrel and umbrella interface adhesive selection and bonding process determination," *Insulators Surge Arresters.*, vol. 6, pp. 7–13, 2012.
[27] J. Kajtna, B. Alič, M. Krajnc, and U. Šebenik, "Influence of hydrogen bond on rheological properties of solventless UV crosslinkable pressure sensitive acrylic adhesive prepolymers," *Int. J. Adhes. Adhesives*, vol. 49, no. 2, pp. 103–108, Mar. 2014. doi: 10.1016/j.ijadhadh.2013.12.016.
[28] A. A. Markou and G. D. Manolis, "Mechanical formulations for bilinear and trilinear hysteretic models used in base isolators," *Bull. Earthquake Eng.*, vol. 14, no. 12, pp. 3591–3611, 2016.
[29] W. D. Iwan and L. D. Lutes, "Response of the bilinear hysteretic system to stationary random excitation," *J. Acoust. Soc. Amer.*, vol. 43, no. 3, pp. 545–552, May 1968. doi: 10.1121/1.1910864.
[30] P. Hu, M. Jiang, C. Huang, and Q. Yu, "Research on interface property of silicon coupling agent," *Surf. Technol.*, vol. 33, no. 5, pp. 19–21, 2004.
[31] D. W. Marhefka and D. E. Orin, "Simulation of contact using a nonlinear damping model," in *Proc. IEEE Int. Conf. Robot. Autom.*, vol. 2, Minneapolis, MN, USA, Apr. 1996, pp. 1662–1668.
[32] C. Potthast, J. Twiefel, and J. Wallaschek, "Modelling approaches for an ultrasonic percussion drill," *J. Sound Vib.*, vol. 308, nos. 3–5, pp. 405–417, Dec. 2007.
[33] W. Xu, C. Li, X. Yue, and H. Rong, "Stochastic responses of a vibro-impact system with additive and multiplicative colored noise excitations," *Int. J. Dyn. Control*, vol. 4, no. 4, pp. 393–399, 2016.
[34] C. Zhaojiang, Z. Shuyi, and Z. Kai, "Nonlinear vibration in metal plate excited by high-power ultrasonic pulses," (in Chinese), *Acta Physica Sinica*, vol. 59, no. 6, pp. 4071–4083, 2010.
[35] M. F. Hamilton, D. T. Blackstock, and L. A. Ostrovsky, "Nonlinear acoustics," *J. Acoust. Soc. Amer.*, vol. 105, no. 2, p. 578, 1974.

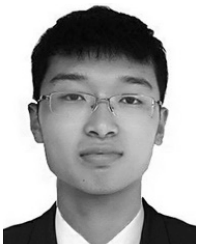

SIDA ZHANG was born in Shandong, China, in 1993. He received the B.S. degree in electrical engineering and automation from Chang'an University, Xi'an, China, in 2012. He is currently pursuing the Ph.D. degree in electrical engineering from Chongqing University, Chongqing, China. His research interests include nondestructive testing and HV outdoor insulation.

CHENJUN GUO was born in Yunnan, China, in 1988. He received the B.S. and M.S. degrees in high voltage engineering from the Department of Electrical Engineering, Tsinghua University, Beijing, China, in 2011 and 2013, respectively. He is currently an Engineer with the Yunnan Electric Power Research Institute, Yunnan Power Grid Company Ltd. His research interests include high voltage test, transformer fault diagnosis, high voltage insulation, and the evaluation of external insulation state.

LI CHENG was born in Chongqing, China, in 1989. He received the B.Sc. and Ph.D. degrees from the Department of Electrical Engineering, Tsinghua University, China, in 2011 and 2016, respectively. He is currently a Lecturer with Chongqing University. His research interests include nondestructive testing and HV outdoor insulation.

HANQING WANG was born in Shandong, China, in 1996. He received the B.S. degree in electrical engineering from Chongqing University, Chongqing, China, in 2018, where he is currently pursuing the Ph.D. degree in condition monitoring of power equipment.

RUIJIN LIAO was born in Suining, Sichuan, China, in 1963. He received the B.S. degree from Xi'an Jiaotong University, in 1988, and the Ph.D. degree from Chongqing University, in 2003, where he is currently a Professor. His research interests include estimation of the electrical equipment and online monitoring technical for the power grid.